Strong suppression of the resistivity near the transition to superconductivity in narrow micro-bridges in external magnetic fields

Xiaofu Zhang,[1] Adriana E. Lita,[2] Konstantin Smirnov,[3,4] HuanLong Liu,[1] Dong Zhu,[1] Varun B. Verma,[2] Sae Woo Nam,[2] and Andreas Schilling[1]

[1]*Department of Physics, University of Zürich, Winterthurerstrasse 190, 8057 Zürich, Switzerland*

[2]*National Institute of Standards and Technology, 325 Broadway, Boulder CO 80305, USA*

[3]*Moscow State Pedagogical University, Malaya Pirogovskaya str. 22, Moscow 127055, Russia*

[4]*National Research University Higher School of Economics, Myasnitskaya str. 20, Moscow 101000, Russia*

We have investigated a series of superconducting bridges based on homogeneous amorphous WSi and MoSi films, with bridge widths w ranging from 2 μm to 1000 μm and film thicknesses $d \sim 4-6$ nm and 100 nm. Upon decreasing the bridge widths below the respective Pearl lengths, we observe in all cases distinct changes in the characteristics of the resistive transitions to superconductivity. For each of the films, the resistivity curves R(B,T) separate at a well-defined and field-dependent temperature $T^*(B)$ with decreasing the temperature, resulting in a dramatic suppression of the resistivity and a sharpening of the transitions with decreasing bridge width w. The associated excess conductivity in all the bridges scales as $1/w$, which may suggest the presence of a highly conducting region that is dominating the electric transport in narrow bridges. We argue that this effect can only be observed in materials with sufficiently weak vortex pinning.

It is generally accepted that the superconductivity in superconducting bridges can be suppressed by gradually reducing their dimensions. While sufficiently thick and wide bridges reflect the properties of the bulk material, wide strips with a reduced thickness $d \lesssim \xi$ (where ξ is the Ginzburg-Landau coherence length) can be viewed as quasi two-dimensional [1]. Their properties are then strongly influenced by the thickness *d*, with a certain reduction of the transition temperature to a zero-resistance state [2-5]. Upon further narrowing a bridge down towards to the one-dimensional (1D) limit $w < \xi$, the critical temperature T_c decreases exponentially with the inverse of the cross section of the bridges [6], leading to a transition to insulating state in the 1D limit [6-10].

Placing a type-II superconducting strip into an external magnetic field, magnetic-field-induced vortices can exist as long as $w > 4.4\ \xi$ [11]. In very thin films, vortices can interact in a different way than in their bulk peers, namely via their stray fields in the surrounding space. The characteristic length scale for this interaction is given by the Pearl length $\Lambda = 2\lambda_L^2/d$, which can be substantially larger than the London penetration depth λ_L [12]. In wide bridges, where the bridge width w is larger than all length scales that are relevant for superconductivity, the vortex-vortex interactions are long-range logarithmic as a function of distance r for $r < \Lambda$, and they determine the superconducting properties in clean enough samples. It has been suggested that in narrow bridges $w < \Lambda$, the vortex-vortex interaction becomes short-range exponential for vortex-vortex separations $r > w/\pi$ [13], thereby excluding a Berezinskii-Kosterlitz-Thouless (BKT) transition [14,15]. While in this low-field limit, surface barriers also play an important role [16], they are negligible in the high-field limit $B \sim B_{c2}$. In this letter we study the transition to superconductivity for amorphous superconducting films in this high-field limit, as a function of the bridge width w for $w < \Lambda$ and $w > \Lambda$.

We have fabricated micro-bridges based on four amorphous WSi and MoSi films of various thickness, with ten different bridge widths w ranging from 2 μm to 1000 μm (fabrication details are provided in the Supplemental Material [17]), and performed detailed transport measurements on them. Figure 1 shows the respective resistive transitions to the superconducting states in magnetic fields up to B = 5 T perpendicular to the films. To facilitate a comparison, the original resistance data have been converted to the respective sheet resistances R_s. In order to eliminate any minor remaining variations in R_s in the normal state due to uncertainties in the geometric dimensions, we normalized the data to the normal-state sheet-resistance values (R_n) of the 100-μm-wide bridges at T = 7 K (T = 10 K for the 6.2-nm-MoSi film) and B = 0 T.

The bridges prepared from the 100-nm-thick WSi film have a zero-field critical temperature $T_c(0) \approx$ 4.95 K, which is close to the maximum T_c for amorphous WSi [18-21], thereby guaranteeing the high quality of our films. The corresponding critical temperature of the 4-nm-thick WSi film is reduced to $T_c(0) \approx$ 3.42 K, in agreement with Refs. [18-21]. The 6.2-nm- and 4.5-nm-thin MoSi films show $T_c(0) \approx$ 6.85 K and 5.15 K**,** respectively, which are the highest reported values for MoSi films in this thickness range to the best of our knowledge [22]. The material parameters relevant for

superconductivity for these four films are tabulated in section S2 in the Supplemental Material [17]. In zero magnetic field (B = 0 T), all bridges made from a particular film show the same critical temperature and temperature dependence of $R_S(T)$ because the respective coherence lengths are more than three orders of magnitude smaller than the width of the narrowest 2-μm-wide bridge [17,23].

With increasing magnetic field, the sheet resistance curves $R_S(B,T)$ are significantly broadened with a resistive "tail", and the transitions are shifted towards lower temperatures along with the reduction of the respective critical temperatures $T_c(B)$. The $R_S(B,T)$ data of the bridges made from the 100-nm-thick WSi film show a shoulder-like drop with decreasing temperature before zero resistance is reached, with a sharp peak in the corresponding derivatives $\mathrm{d}R_S/\mathrm{d}T$ (see Fig. 2). This feature is particularly pronounced in the wide bridges, but vanishes for $B \to B_{c2}$ and when the bridge width is far smaller than the Pearl length. It is reminiscent of corresponding drops in $R_S(B,T)$ that have been attributed to a first-order solidification of a vortex fluid to a vortex lattice in high-temperature superconductors [23]. While this observation is not the central subject of this letter, its occurrence is a strong indication for the high quality of our films and supports the notion that bulk vortex pinning in amorphous superconducting films is weak enough to allow for the occurrence of this transition [24].

All our data show a further unexpected striking phenomenon: upon lowering the temperature, the $R_S(B,T)$ data of the bridges for a particular film and magnetic field separate in such a way that the resistivity in narrow bridges is significantly suppressed near the transition, thereby leading to a narrowing of the transition to the zero-resistance state (Fig. 1). For each of the films, this separation occurs at a well-defined, field-dependent temperature $T^*(B)$ [see Fig. 3(a) as an example]. It coincides with the temperature where the derivatives dR_s/dT for a given film and magnetic field for the different bridge widths w show a sharp maximum [Fig. 3(b)], indicating that there is a change in the dissipative mechanism for electric-current flow. We shall see below that a nonlinear current-voltage characteristic also sets in around $T^*(B)$. As this temperature is independent of the bridge width, we may interpret it as an intrinsic temperature $T^*(B)$ of the film where the electric currents are immune to geometric effects or any vortex-pinning mechanisms.

For an interpretation of the observed change in the characteristics of $R_s(B,T)$ we first state that the reduction in $R_s(B,T)$ cannot be explained by the presence of conventional surface barriers [16]. It is known that such barriers inhibit dissipative vortex flow transverse to the current and therefore result

in a reduction of the resistance. The maximum magnetic field below which surface barriers can play a role is given by the superheating field B_s, which is in the limit $\kappa >> 1$ given by $B_s \approx \phi_0/(4\pi\xi\lambda)$ [25]. It amounts to ≈ 73 mT at most in our case [17] and is probably much smaller close to the critical temperature, where both λ_L and ξ diverge. As $B \gg B_s$ in our investigations, with no signs of any weakening of the effect in the limit $B \to B_{c2}$, we definitely conclude that conventional surface barriers are not responsible for the reduction of in $R_s(B,T)$.

Most interestingly, a qualitatively similar sharpening of the resistivity in ~ 300-µm-wide strips of superconducting $Bi_2Sr_2CaCu_2O_8$ films with thickness $d \approx 13$ µm [26] could be very well explained by the presence of surface barriers. It was reported to be most pronounced around $B \approx 50$ mT but became negligible beyond $B \approx 2$ T. For the respective experiments we estimate with $\lambda_L \approx 190$ nm and $\xi \approx 1$ nm for $Bi_2Sr_2CaCu_2O_8$ [27] a $B_s \lesssim 1$ T, in favorable agreement with the observation that the effect vanished in large enough magnetic fields [26].

To quantify the observed reductions of $R_s(B,T)$ in our experiments, we have determined the temperatures T_{max} where the differences between the resistivities of the 1000 µm and the 2 µm wide films are largest for each film and each magnetic field. In Figs. 4(a)-4(d) we show the evolution of $R_s(T_{max})$ as functions of the bridge width *w*. We can state that the observed reduction of the resistivity as a function of *w* is most prominent below the scale of the Pearl length (with Λ between 8 µm and 345 µm respectively [17]), but becomes almost immeasurably small for *w* > 500 µm > Λ.

We now tentatively interpret the observed reductions in resistivity as being a result of the appearance of an additional conductivity channel. The $R_s(B,T)$ data for *w* = 1000 µm and *w* = 500 µm are hardly distinguishable, and we therefore use the resistivity of the widest bridge (*w* = 1000 µm) of each film as a reference representing the value for an infinite film of equal thickness. We can plot this additional conductivity for a given bridge width *w* at $T = T_{max}$, $\Delta\sigma(T_{max},w) = \sigma(T_{max},w) - \sigma(T_{max}, w = 1000\ \mu\text{m})$ as a function of *w* for different magnetic fields [see Figs. 4(e)-4(h)]. For these plots we normalized the conductivities to the respective values R_n. As a general trend, these additional conductivities scale in all cases almost exactly as $1/w$ over at least 2 decades. We note that similar analyses for $T \neq T_{max}$ yield the same $1/w$-type of scaling of $\Delta\sigma(T,w)$. In view of this peculiar width dependence, we may adopt a simple phenomenological model where we assume the presence of a localized region along the strip with width-independent size $s < w$ exhibiting a higher conductivity σ_s than the rest of the film with conductivity σ_0. Then, the averaged conductivity measured in an

experiment is

$$\sigma_{av} = [s\sigma_s + (w - s)\sigma_0]/w = \sigma_0 + s(\sigma_s - \sigma_0)/w. \quad (1)$$

The corresponding excess conductivity $\sigma_{av} - \sigma_0$ scales as $1/w$ for a given film and magnetic field B, and vanishes for an infinite film, with $\sigma_{av} = \sigma_0$. As long as the spatial variation of $\sigma(x)$ from $\sigma = \sigma_s$ to $\sigma = \sigma_0$ occurs over a short enough length scale $s \ll w$, this result is insensitive to how exactly $\sigma(x)$ varies from $x = 0$ to $x > s$. Any deviations from a $1/w$-scaling for small bridge widths would indicate that w becomes comparable to s, and the measured conductivity would eventually saturate at $\sigma_s > \sigma_0$ for even smaller values of w. As we do not see any deviation from this scaling even for the narrowest bridges, the length scale s within this model (which may depend on magnetic field) must be smaller than 2 μm, both in the thick and in the thin films.

The fact that there exists a separation of the $R_s(B,T)$ data even in large magnetic fields calls for a discussion of possible vortex-pinning effects that are responsible for the reduction of the resistance. The observation of a non-linear *I-V* in the mixed state of superconductors at low currents is in most cases associated with vortex pinning or, more generally, with the presence of potential barriers inhibiting vortex motion [28]. Indeed, the current-voltage (*I-V*) characteristics start to deviate from linearity around the characteristic temperature $T^*(B)$ below which the reduction of the resistance sets in. While hardly discernible in the wide bridges, the data taken on the 2-μm-wide bridge made of the 4.5-nm-thick MoSi film show that the respective *I-V* curves are linear above $T^* \approx 4.4$ K in B = 2 T, and become increasingly non-linear below it (the *I-V* curves near the transition regime are provided in Fig. S2 in the Supplemental Material [17]). As we do not expect any width-dependent change of the physical properties across the bulk of the film during the structuring process, we may ascribe the source of the non-linear *I-V* to a localized region, most likely located along the edges of the bridges, with properties that are independent of the bridge width. This scenario would be compatible with the 1/w scaling of the excess conductivity and the presence of a narrow, highly conductive channel along the bridge edges. While this scenario can semi-quantitatively explain our data very well, crucial information about the extension s of such channels and the microscopic details of the respective current-transport mechanism are yet to be clarified, however.

We note that both the vortex structure and the vortex interactions for $w < \Lambda$ may be entirely

different from those in infinite films [13,29]. At present, it has, to our knowledge, not yet been considered how such arguments can be transferred to the case of a dense lattice of Pearl vortices with $r < w \ll \Lambda$ and $B \to B_{c2}$, nor what the possible consequences on measurable quantities might be. However, it is conceivable that a reduced vortex interaction among Pearl vortices in narrow enough bridges [13] makes them much more susceptible to pinning, or that peculiarities near the edges of a bridge [29] can play an important role.

Finally we argue that the features reported here can only be observed in films of weakly-pinning superconductors. In Fig. 5, we show corresponding $R_S(B,T)$ data taken on a thin film ($d \approx 5$ nm) of NbN, which is known to be a strongly-pinning superconductor [30]. It is obvious that the field-induced large reduction in resistivity as we measured it in the WSi and MoSi films is absent. We believe that if bulk pinning is strong enough, any additional, comparably weak increase of the electrical conductivity at the bridge edges is dominated by bulk pinning and therefore becomes unobservable.

In conclusion, we have shown that the resistive transitions in thin films of the weakly-pinning amorphous superconductors WSi and MoSi in a magnetic field are strongly dependent on the width of the samples, with a substantial narrowing near the critical temperatures as soon as the bridge widths become much less than the corresponding Pearl lengths. The $1/w$ scaling of the excess conductivity suggests the existence of highly conducting narrow channels along the edges of the bridges. While this effect may not be observable in thin films of strongly-pinning superconductors, it may turn out to be crucial for the interpretation of resistance data taken on thin films of amorphous superconductors in large magnetic fields.

Acknowledgements

H. Liu and D. Zhu are supported by the Schweizerische Nationalfonds zur Förderung der Wissenschaftlichen Forschung (grant No. 20-175554). K. Smirnov thanks the Russian Science Foundation (RSF) Project No. 18-12-00364. We thank to Prof. V. G. Kogan for stimulating discussions.

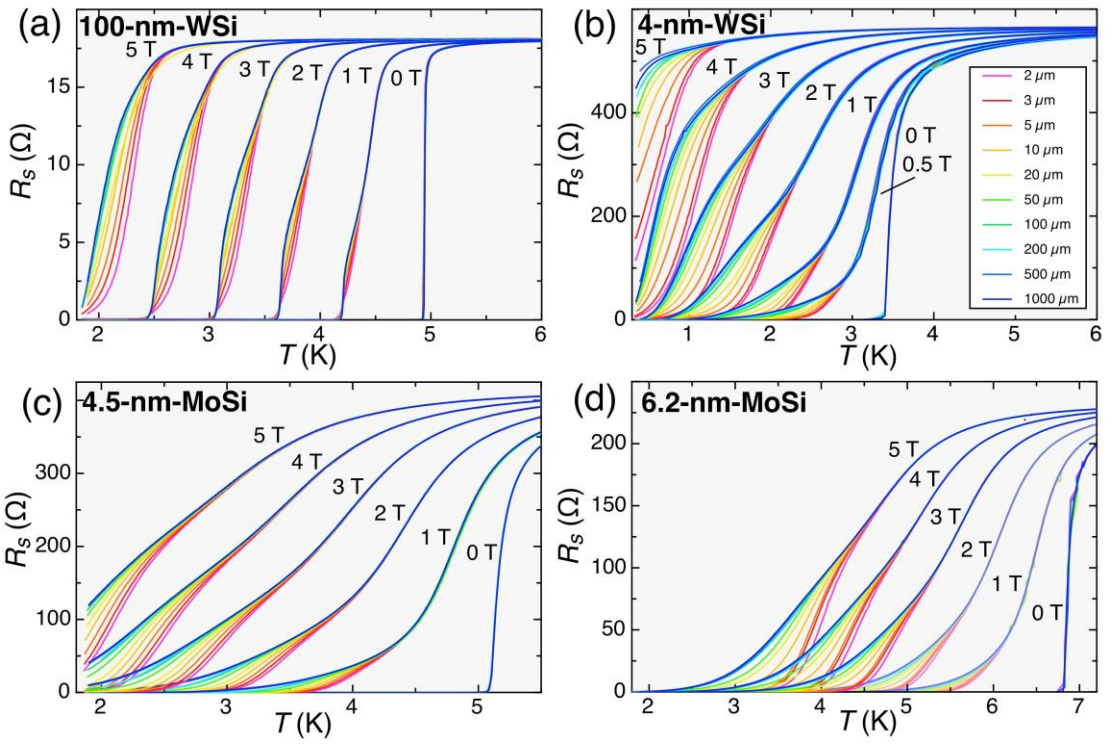

FIG. 1. The sheet resistance R_s as a function of temperature in magnetic fields ranging from $B = 0$ T to $B = 5$ T for 100-nm-thick WSi (a), 4-nm-thick WSi (b), 4.5-nm-thick MoSi (c), and 6.2-nm-thick MoSi (d).

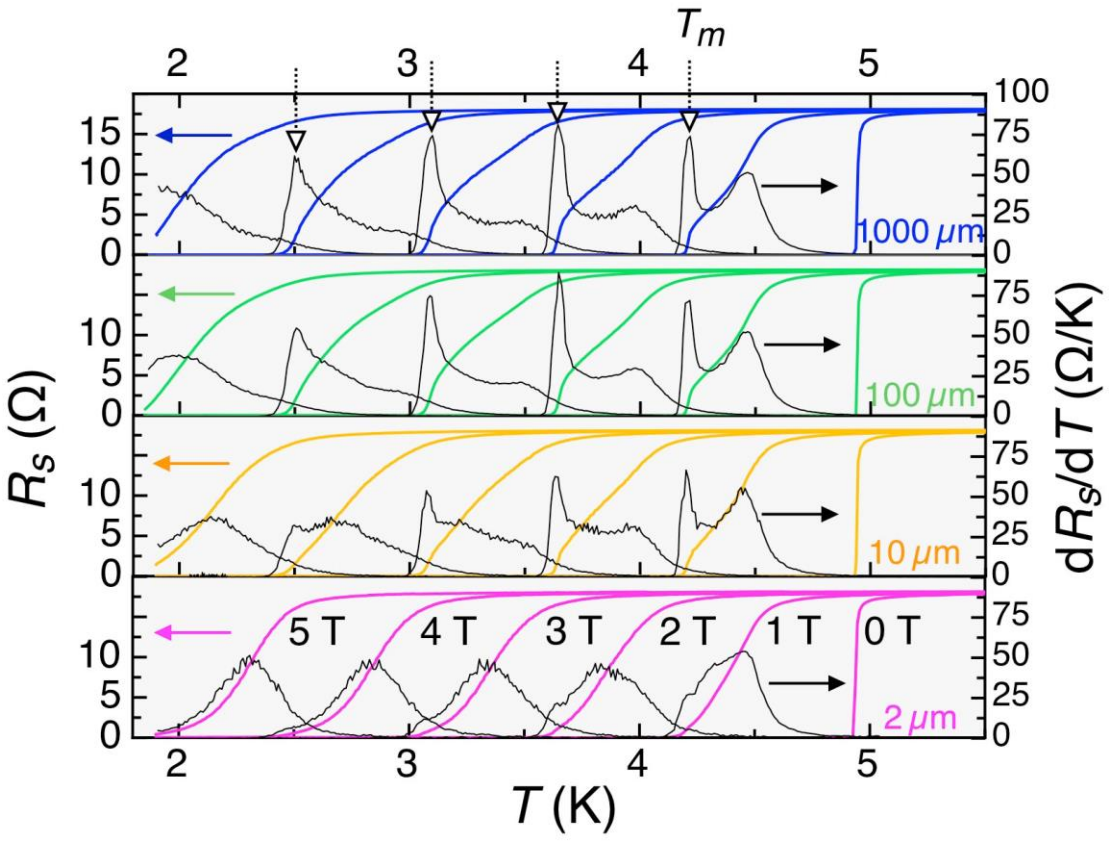

FIG. 2. Temperature dependence of the sheet resistance $R_s(B,T)$ of the 100-nm-thick WSi film for different bridge widths w, in magnetic fields between B = 0 T and 5 T (colored curves, left scales). The black curves represent the corresponding derivatives $\mathrm{d}R_s/\mathrm{d}T$ (right scales). The dotted arrows indicate sharp drops in the resistivity that can be attributed to a vortex-lattice melting transition.

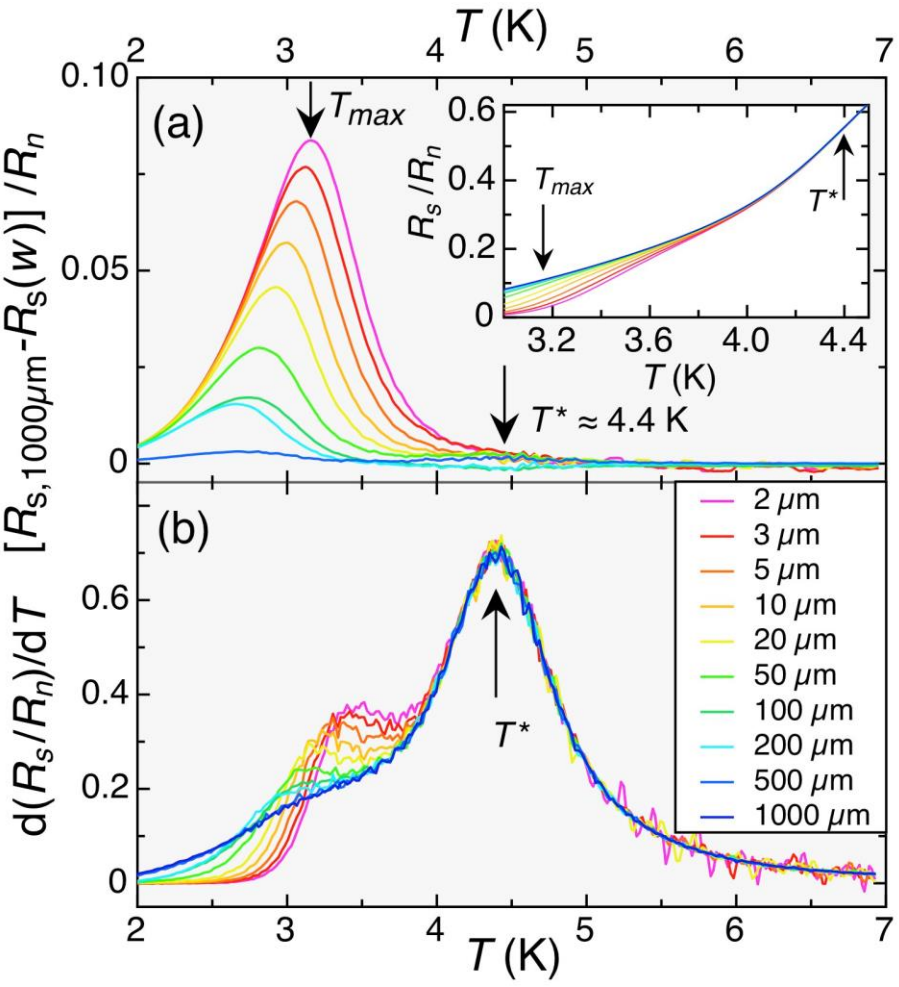

FIG. 3. (a) Difference in the normalized sheet resistance between the 1000 μm wide bridge and the other bridges of the 4.5 nm thin MoSi film in $B = 2$ T. T^* denotes the temperature around which this difference vanishes and all resistance curves merge (inset), while T_{max} indicates the temperature where the difference between the 1000 μm and the 2 μm data is largest. (b) The derivative of the normalized sheet resistance, showing a sharp maximum at T^*.

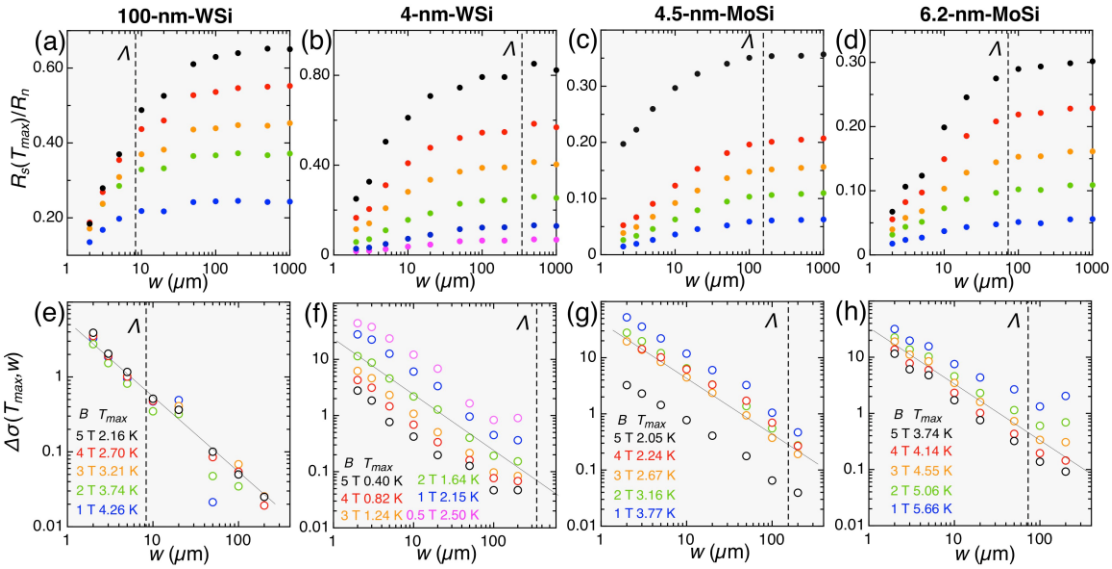

FIG. 4. (a)-(d) Evolution of the normalized sheet resistances as functions of the respective bridge width w in magnetic fields between B = 1 T (blue filled circles, lowest curves) and B = 5 T (black filled circles, highest curves), in steps of 1 T. The data have been taken at the temperatures T_{max} where the difference between the 1000 μm and the 2 μm data are largest [see Fig. 3(a)]. (e)-(h) Excess normalized conductivities $\Delta\sigma(T_{max}, w)$ relative to the values of the 1000-μm-wide bridges at the respective temperatures T_{max}, as functions of the bridge width w. The thin solid lines represent a $1/w$ scaling and are to guide the eye. The respective Pearl lengths Λ are indicated as vertical dashed lines.

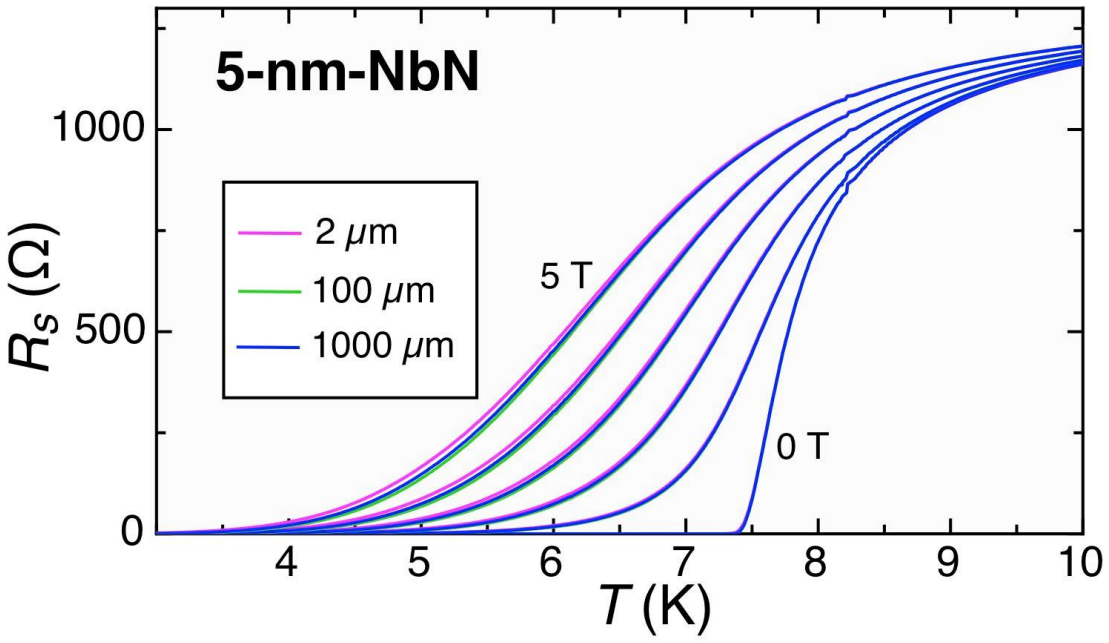

FIG. 5. The sheet resistance R_s as a function of temperature for bridges made from a 5-nm-thick NbN film, in magnetic fields between $B = 0$ T to $B = 5$ T in steps of 1 T. No reduction in resistivity is visible upon decreasing the bridge width from 1000 μm to 2 μm.

References

[1] M. Tinkham, Introduction to Superconductivity (McGrawHill, New York, 1975) (reprinted by R. E. Krieger, Malabar, 1980).

[2] M. Strongin, R. S. Thompson, O. F. Kammerer, and J. E. Crow, Phys. Rev. B **1**, 1078 (1971).

[3] S. A. Wolf, J. J. Kennedy, and M. Nisenoff, J. Vac. Sci. Technol. **13**, 145 (1976).

[4] Y. Oreg and A. M. Finkel'stein, Phys. Rev. Lett. **83**, 191 (1999).

[5] J. M. Graybeal and M. R. Beasley, Phys. Rev. B **29**, R4167 (1984).

[6] H. Kim, S. Jamali, and A. Rogachev, Phys. Rev. Lett. **109**, 027002 (2012).

[7] A. Bezryadin, C. N. Lau & M. Tinkham, Nature **404**, 971 (2000).

[8] A. T. Bollinger, R. C. Dinsmore, III, A. Rogachev, and A. Bezryadin, Phys. Rev. Lett. **101**, 227003 (2008).

[9] A. T. Bollinger, A. Rogachev, M. Remeika, and A. Bezryadin Phys. Rev. B 69, **180503(R)**, (2004).

[10] D. Meidan, Y. Oreg, and G. Refael, Phys. Rev. Lett. **98**, 187001 (2007).

[11] K. K. Likharev, Rev. Mod. Phys. **51**, 101 (1979).

[12] J. Pearl, Appl. Phys. Lett. **5**, 65 (1964).

[13] V. G. Kogan, Phys. Rev. B **75**, 064514 (2007).

[14] V. L. Berezinskii, Zh. Eksp. Teor. Fiz. **61**, 1144 (1971) [Sov. J. Exp. Theor. Phys. **34**, 610 (1972)].

[15] J. M. Kosterlitz and D. J. Thouless, J. Phys. C **6**, 1181 (1973).

[16] C. P. Bean and J. D. Livingston, Phys. Rev. Lett. **12**, 14 (1964).

[17] See Supplemental Material at XXX for (i) more information on the fabrications of these bridges, (ii) the material parameters of the investigated films (iii) temperature-dependent *I*-*V* curves in $B = 2$ T for MoSi bridges with $d = 4.5$ nm.

[18] S. Kondo, J. Mater. Res. **7**, 853 (1992).

[19] X. Zhang, A. Engel, Q. Wang, A. Schilling, A. Semenov, M. Sidorova, H.-W. Hübers, I. Charaev, K. Ilin, and M. Siegel Phys. Rev. B **94**, 174509, (2016).

[20] B. Baeka, A. E. Lita, V. Verma, and S. W. Nam, Appl. Phys. Lett. **98**, 251105 (2011).

[21] X. Zhang, A.E. Lita, M. Sidorova, V.B. Verma, Q. Wang, S. Woo Nam, A. Semenov, and A. Schilling, Phys. Rev. B **97**, 174502 (2018).

[22] A. Banerjee, L. J. Baker, A. Doye, M. Nord, R. M. Heath, K. Erotokritou, D. Bosworth, Z. H. Barber, I. MacLaren and R. H. Hadfield, Supercond. Sci. Technol. **30**, 084010 (2017).

[23] W. K. Kwok, S. Fleshler, U. Welp, V. M. Vinokur, J. Downey, G. W. Crabtree, and M. M. Miller, Phys. Rev. Lett. **69**, 3370 (1992).

[24] I. Roy, S. Dutta, A. N. R. Choudhury, S. Basistha, I. Maccari, S. Mandal, J. Jesudasan, V. Bagwe, C. Castellani, L. Benfatto, and P. Raychaudhuri, Phys. Rev. Lett. **122**, 047001 (2019).

[25] J. R. Clem, in Proceedings of the 18th Conference on low Temperature Physics (LT 13), edited by K.D. Timmerhaus, W. J. O' Sullivan, and E. F. Hammel (Plenum, New York, 1974), Vol. 3, p. 102.

[26] D. T. Fuchs, R. A. Doyle, E. Zeldov, S. F. W. R. Rycroft, T. Tamegai, S. Ooi, M. L. Rappaport, and Y. Myasoedov, Phys. Rev. Lett. **81**, 3944 (1998).

[27] E. F. Talantsev and J. L. Tallon, Nature Comms. **6**, 8820 (2015).

[28] F. Tafuri, J. R. Kirtley, D. Born, D. Stornaiuolo, P. G. Medaglia, P. Orgiani, G. Balestrino, and V. G. Kogan, Europhys. Lett. **73**, 948 (2006).

[29] V. G. Kogan, Phys. Rev. B. **49**, 15874 (1994).

[30] A. Pruymboom, P. H. Kes, E. van der Drift, and S. Radelaar, Phys. Rev. Lett. **60**, 1430 (1988).

Supplemental Material for "Strong suppression of the resistivity near the transition to superconductivity in narrow micro-bridges in external magnetic fields"

X. Zhang, A.E. Lita, K. Smirnov, H. Liu, D. Zhu, V.B. Verma, S.W. Nam, and A. Schilling

S1 fabrication of superconducting micro-bridges

The superconducting thin films adopted in our research were prepared by magnetron sputtering deposition. The WSi films was deposited by co-sputtering from W and Si targets in 1.2 mTorr Ar pressure, on oxidized Si substrate. The sputtering powers for W and Si guns was 100 W and 180 W, respectively. The WSi film was *in situ* capped with 2 nm sputtered amorphous Si film. The WSi film had a nominal Si content of ~ 25% and consists of an amorphous structure as verified by x-ray diffraction (XRD) and high-resolution transmission electron microscopy (TEM).

The 4.5-nm- and 6.2-nm-thick MoSi films were sputtered from a $Mo_{0.8}Si_{0.2}$ in 3.5 mTorr and 2.5 mTorr Ar pressure, respectively. The sputtering power for the MoSi gun was 225 W. The MoSi films were in-situ capped with 3 nm sputtered amorphous SiO_2 films. The MoSi films had a nominal amorphous

structure as verified by x-ray diffraction.

We firstly patterned the Ti/Au contacts on the as-grown films by lift-off technique. Then the micro-bridges were defined by optical lithography, followed by reactive ion-etching. The bridge widths range from 2 μm to 1000 μm, as it is shown in Fig. S1 for the 4.5-nm-MoSi film. The bridges are electrically connected in a four-wire configuration by wire bonding (white spots on top of the gold contacts, see Fig. S1) for the transport measurement (Physical properties measurement system, *Quantum Design Inc.*).

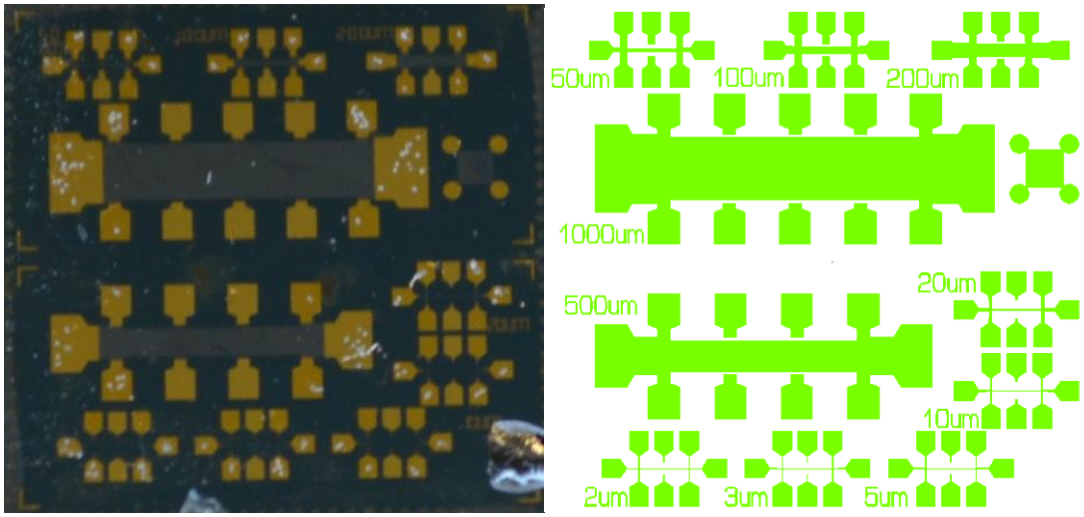

Fig. S1. Left: Image of the ten micro-bridges from the MoSi film with d = 4.5 nm. The area shown is 10 mm × 10 mm. Right: A schematic diagram of the distributions of the ten micro-bridges.

S2 Material parameters of the investigated microbridges

Zero-field critical temperatures $T_c(0)$ of the investigated films. The Ginzburg-Landau coherence lengths $\xi_{GL}(0)$, London penetration depths $\lambda_L(0)$, Pearl lengths $\Lambda(0)$, superheating fields B_s, and upper-critical fields $B_{c2}(0)$ are all extrapolated to $T = 0$. While ξ_{GL} was derived from an estimate of B_{c2} based on resistance measurements, λ_L was obtained by the procedure described in Ref. [19].

material	d (nm)	$T_c(0)$ (K)	$\xi_{GL}(0)$ (nm)	$\lambda_L(0)$ (nm)	$\Lambda(0)$ (μm)	B_s (mT)	$B_{c2}(0)$ (T)
WSi	4	3.42	7.80	830	345	25	5.40
WSi	100	4.95	6.14	645	8.3	42	8.60
MoSi	4.5	5.15	5.31	590	155	53	11.69
MoSi	6.2	6.85	4.73	475	73.6	73	14.70
NbN	5	7.85	4.75	750	225	46	20.59

S3 The current-voltage characteristics near the transition to superconductivity

The *I-V* curves of two 4.5-thick MoSi films (w = 1000 μm and 2 μm, $T_c \approx 4.95$ K) were collected between 3 K to 5 K [Figs. S2(a) and (b)]. A non-linear *I-V* characteristics appears for temperatures below $T^* \approx 4.4\ K$. Figs. S2(c) shows the normalized dV/dI curves in the zero-current limit for w = 2 μm, which further illustrates the onset of a nonlinear current-voltage characteristics around T^*.

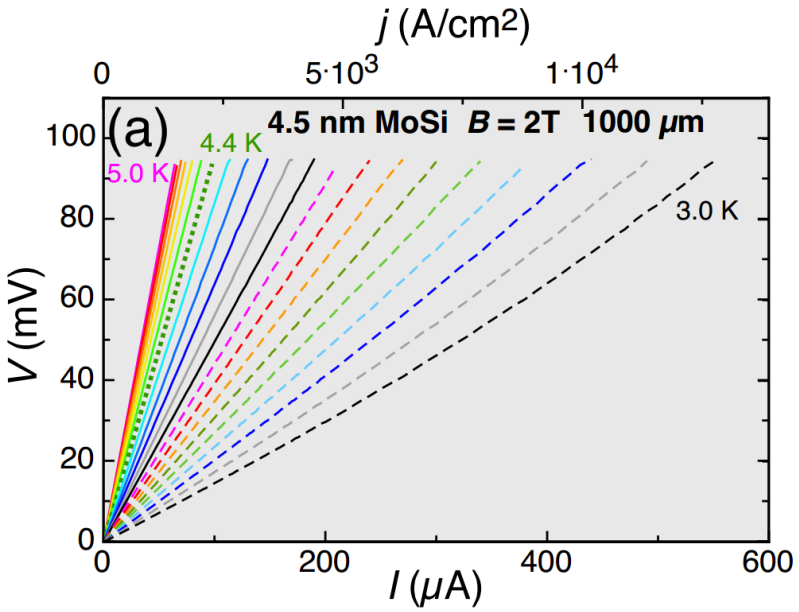

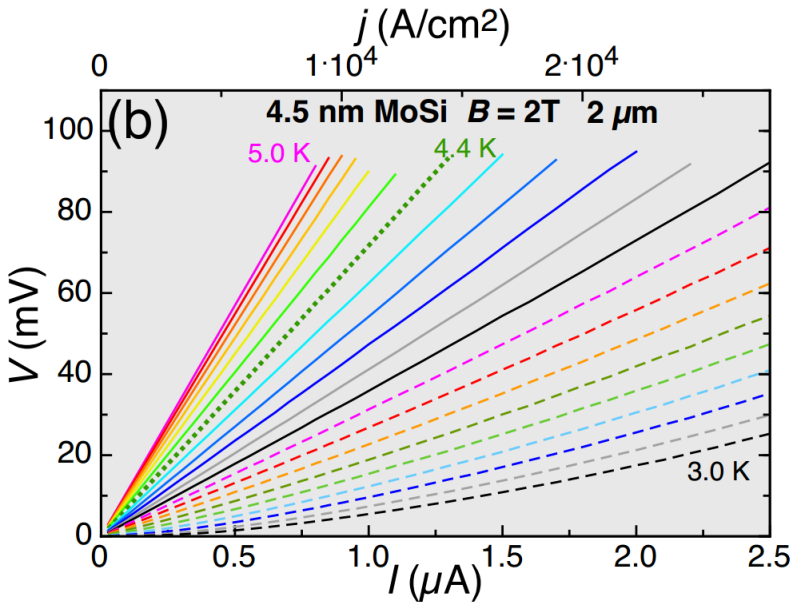

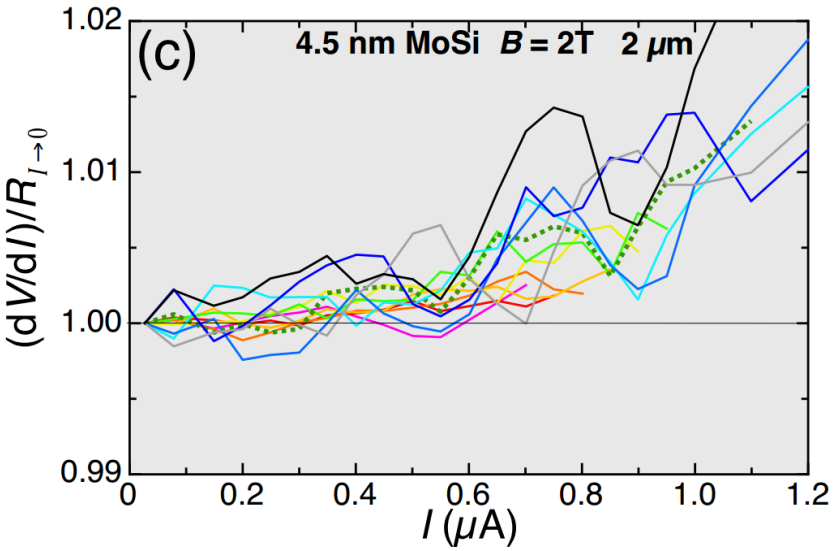

FIG. S2. Current-voltage characteristics for the 1000-μm-wide (a) and 2-μm-wide (b) bridges from the 4.5-nm-thick MoSi films from $T = 3$ K to $T = 5$ K in $B = 2$ T, in steps of 0.1 K. The data at the corresponding temperature $T^* \approx 4.4$ K are marked as a green dotted line. (c) Normalized derivative dV/dI for temperatures around $T \approx T^*$.